Supporting Information for "Global changes water vapor 1979-2020"

Richard P. Allan[1] [*], Kate M. Willett[2], Viju O. John[3], Tim Trent[4]

[1]Department of Meteorology/National Centre for Earth Observations, University of Reading, UK

[2]Met Office Hadley Centre, Exeter, UK

[3]EUMETSAT, Daarmstadt, Germany

[4]School of Physics and Astronomy/National Centre for Earth Observation, University of Leicester, UK

Contents of this file

1. Text S1

2. Figures S1 to S5

3. Tables S1 to S3

Introduction

The supporting information consists of additional supplementary figures.

Text S1.

Additional tables document mean surface and atmospheric relative humidity and temperature (1995-2014; Table S1), trends in atmospheric temperature (1988-2014; Table S2)

———————

[*]Department of Meteorology, University

of Reading, Reading, Berkshire, UK

March 3, 2022, 3:50pm

and sensitivity of atmospheric temperature to surface temperature (1988-2014; Table S3) across models, reanalyses and observational-based products.

Additional supplementary figures referred to in the text are listed below. Fig. S1 shows trends in water vapor (1988-2014) throughout the troposphere. The effect of varying time periods and missing data filling (applying ERA5 values to AIRS or HadISDH) and averaging (deseasonalised percentage anomalies of the global mean "%anoms(Avg)" or global average of grid point deseaonalised percentage anomalies "Avg(%anoms)") is illustrated in Fig. S2. Fig. S3 displays deseasonalised anomalies in water vapor at different atmospheric pressure levels while trends in temperature throughout the troposphere (1988-2014) across datasets (Fig. S4) considered and described in the main paper. Fig. S5 shows how sensitive trends in 400 hPa temperature or water vapor are to the ratio of tropical mean to global mean warming or land mean to global mean warming.

Averaging method: taking averages of grid point anomalies (rather than anomalies of averaged fields) increases the weighting of higher latitude regions with smaller absolute moisture amounts. This tends to increase the interannual sensitivity in the lower troposphere in AIRS, ERA5 and HadISDH yet increase the multi-decadal trends in the upper troposphere in ERA5 suggesting that contrasting regional patterns of changes are operating at the different time-scales (Fig. S2c-d).

Time period: including the post 2014 period increases the water vapor trends in AIRS and ERA5 by about 0.5 to 1 %/decade through most of the troposphere and also increases the interannual sensitivity by about 1%/K in AIRS data and less in ERA5 (Fig. S2a-b). Considering averages of grid point anomalies (rather than anomalies of averaged fields) increases the weighting of higher latitude regions with smaller absolute moisture amounts.

March 3, 2022, 3:50pm

This tends to increase the interannual sensitivity in the lower troposphere in AIRS, ERA5 and HadISDH yet increase the multi-decadal trends in the upper troposphere in ERA5 suggesting that contrasting regional patterns of changes are operating at the different time-scales (Fig. S2c-d).

Missing data: filling of the small amount of missing AIRS data produces little effect while filling of HadISDH missing data only affects the calculation of trends in deseasonalised anomalies of absolute global means: the negative trend in unfilled HadISDH data is an artifact of the changing global sampling while interannual variability and trends show little sensitivity to filling when global averages of deseasonalised grid-point anomalies are computed (Fig. S2c-d). The detrended interannual sensitivities are also robust to sampling since values do not change noticeably between filled and unfilled versions (Fig. S2) of AIRS(/ERA5) and HadISDH(/ERA5). However, without filling, HadISDH global mean q_{2m} trends are substantially more negative $(-1.8\%/K)$ than the filled estimate ($\sim$0 %/K; see Fig. S2) and this aliases onto the interannual relationship without detrending (2 %/K), less than half the detrended estimate (not shown).

Detrending: the interannual relationship between water vapor and surface temperature was computed with and without detrending to assess the sensitivity and dataset dependence. For example, SSMI(S)-ERA5 total $dCWV/dT_s$ (1988-2014) is 5.7 %/K compared with 5.5%/K for detrended estimates. However, for ERA5, which produces elevated water vapor anomalies early in the record, total $dCWV/dT_s = 5.2$ %/K is lower than the detrended estimate of 5.8 %/K. Conversely, model simulations produce a larger total $dCWV/dT_s$ (*amip* 5.6$\pm$0.4 %/K; *historical* 6.4$\pm$1.0 %/K) compared with detrended estimate (*amip* 4.8$\pm$0.5 %/K; *historical* 5.6$\pm$1.4 %/K). In the upper troposphere (300 hPa)

March 3, 2022, 3:50pm

ERA5 and AIRS (2002-2014 only) are consistent (13.5 %/K and 13.4 % without detrending) and slightly greater with detrending (14.4 %/K and 14.3 %/K) while the models simulate a smaller response without detrending (*amip* 13.4±1.50, *historical* 14.1±3.4) compared to with detrending (*amip* 12.5±1.9 %/K, *historical* 13.0±4.8 %/K). This suggests that the physical processes determining water vapor changes on interannual and decadal timescales differ in the simulations while data homogeneity limits the interpretation of the differences between detrended and un-detrended estimates in the observations.

Dewpoint temperature conversion: finally, the effect of computing 2 m specific humidity from monthly 2 m dewpoint and standard air temperature and surface pressure on global means and their changes was estimated by considering April in 1995 and 2019 (both ENSO neutral months). Global mean specific humidity was compared against calculations performed on the 720 hourly fields in the month. The monthly method was found to underestimate global monthly specific humidity computed from hourly data by 1% but the percentage change in global mean from 1995 to 2019 of 2.3% from the hourly data was closely approximated by the monthly method (2.4%). Therefore it was decided that the monthly method is adequate for the purposes of the analysis of relative changes in near-surface water vapor discussed in the main paper.
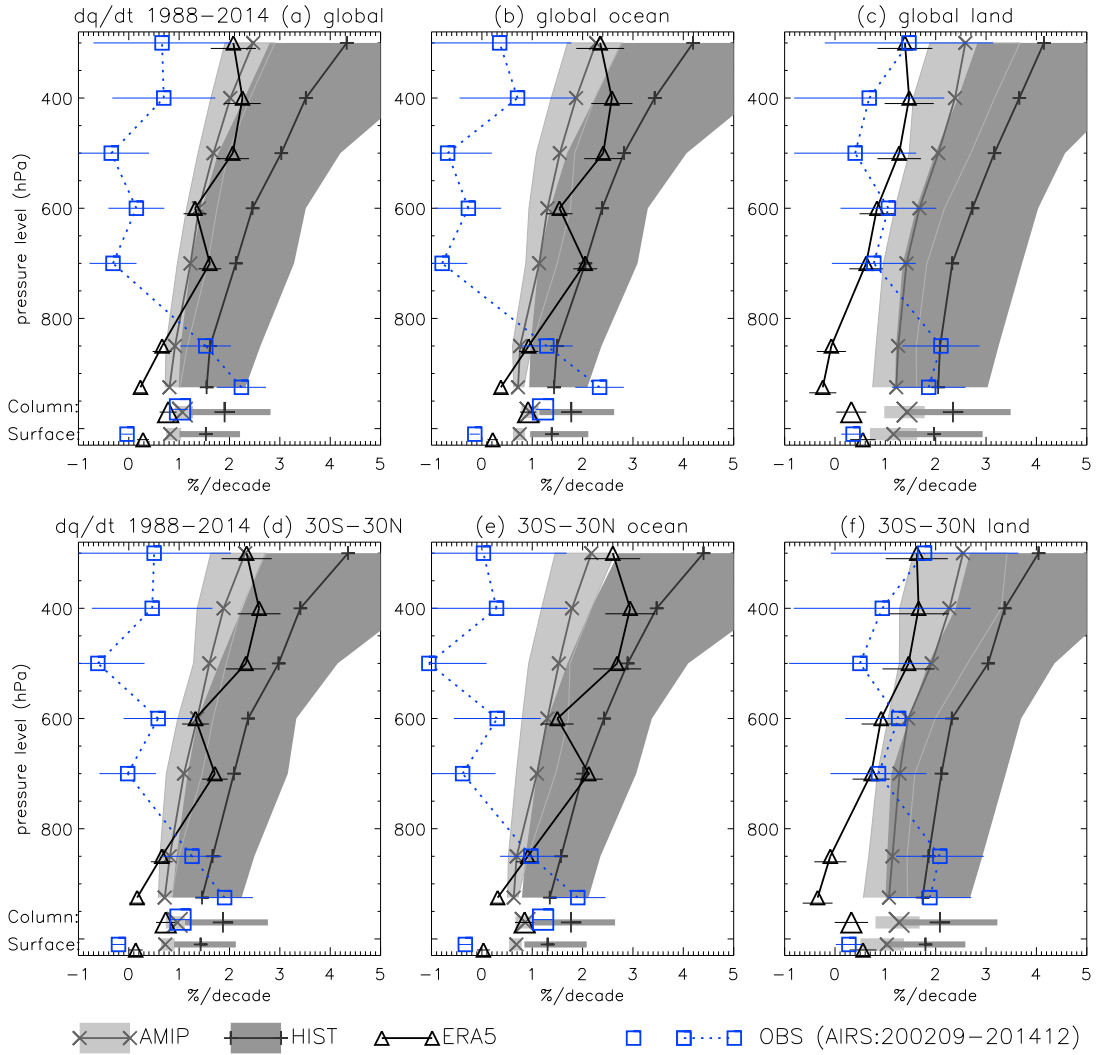
Figure S1. Trends in atmospheric, column integrated and near surface water vapor for the (a) global land and ocean, (b) global ocean, (c) global land, (d) tropical land and ocean, (e) tropical ocean and (f) tropical land over 1988-2014 for *amip* and *historical* model experiments (ensemble median±1 standard deviation), ERA5, AIRS satellite observations (2002-2014), SSMI(S) microwave satellite column integrated water vapor and HadISDH 2 m observations (horizontal lines denote 90% uncertainty range).

March 3, 2022, 3:50pm
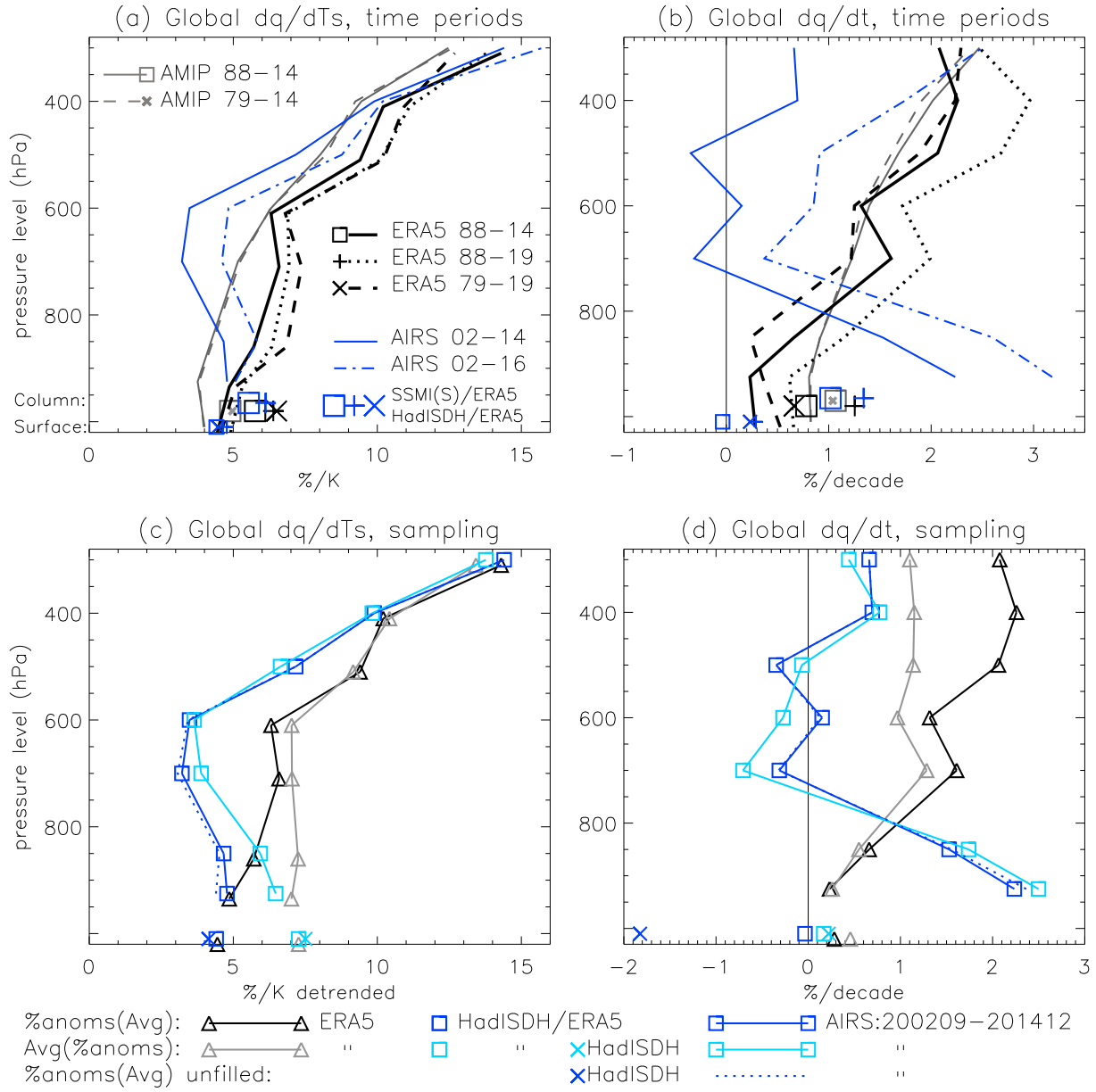
Figure S2.   Effect of varying time periods and filling and averaging on (a,c) interannual sensitivity of specific humidity to surface temperature (dq/dTs) and (b,d) trends in specific humidity (dq/dt) for global averages in ERA5, AIRS and HadISDH datasets, 1988-2014.

March 3, 2022, 3:50pm
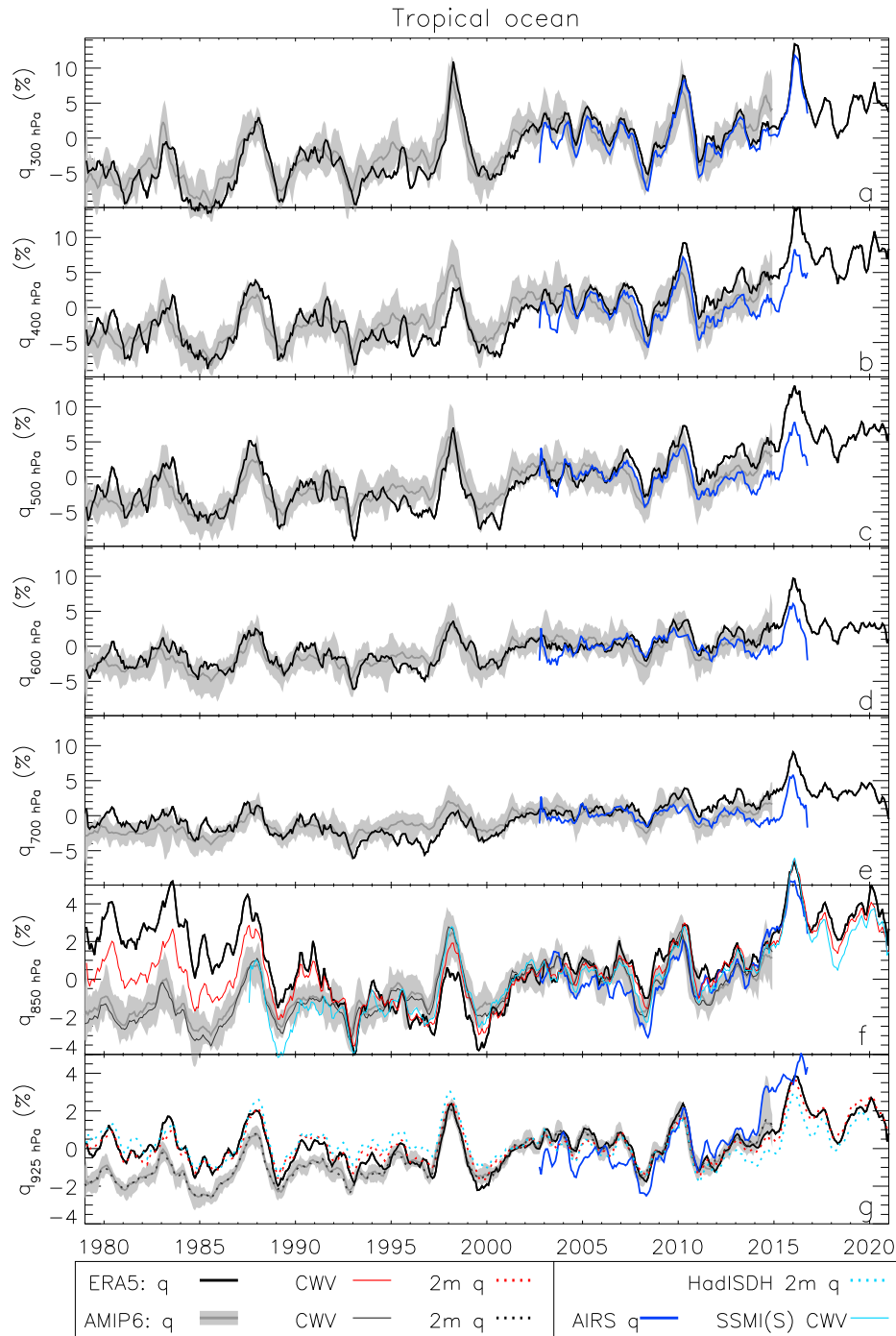
Figure S3.   Deseasonalised anomaly time series of tropical ocean mean atmospheric water vapor (% anomaly relative to 1995-2014 baseline) throughout the atmosphere for *amip* models (ensemble mean±1 standard deviation), ERA5 and AIRS satellite observations at (a) 300 hPa, (b) 400 hPa, (c) 500 hPa, (d) 600 hPa, (e) 700 hPa, (f) 850 hPa and (g) 925 hPa. Also shown in (f) are percentage anomalies in column integrated water vapor from ERA5, AMIP6 and SSMI(S) satellite observations while in (g) percentage anomalies in $2m$ near-surface specific humidity from ERA5, AMIP6 and HadISDH observations are shown. A 5-month smoothing is applied.

March 3, 2022, 3:50pm
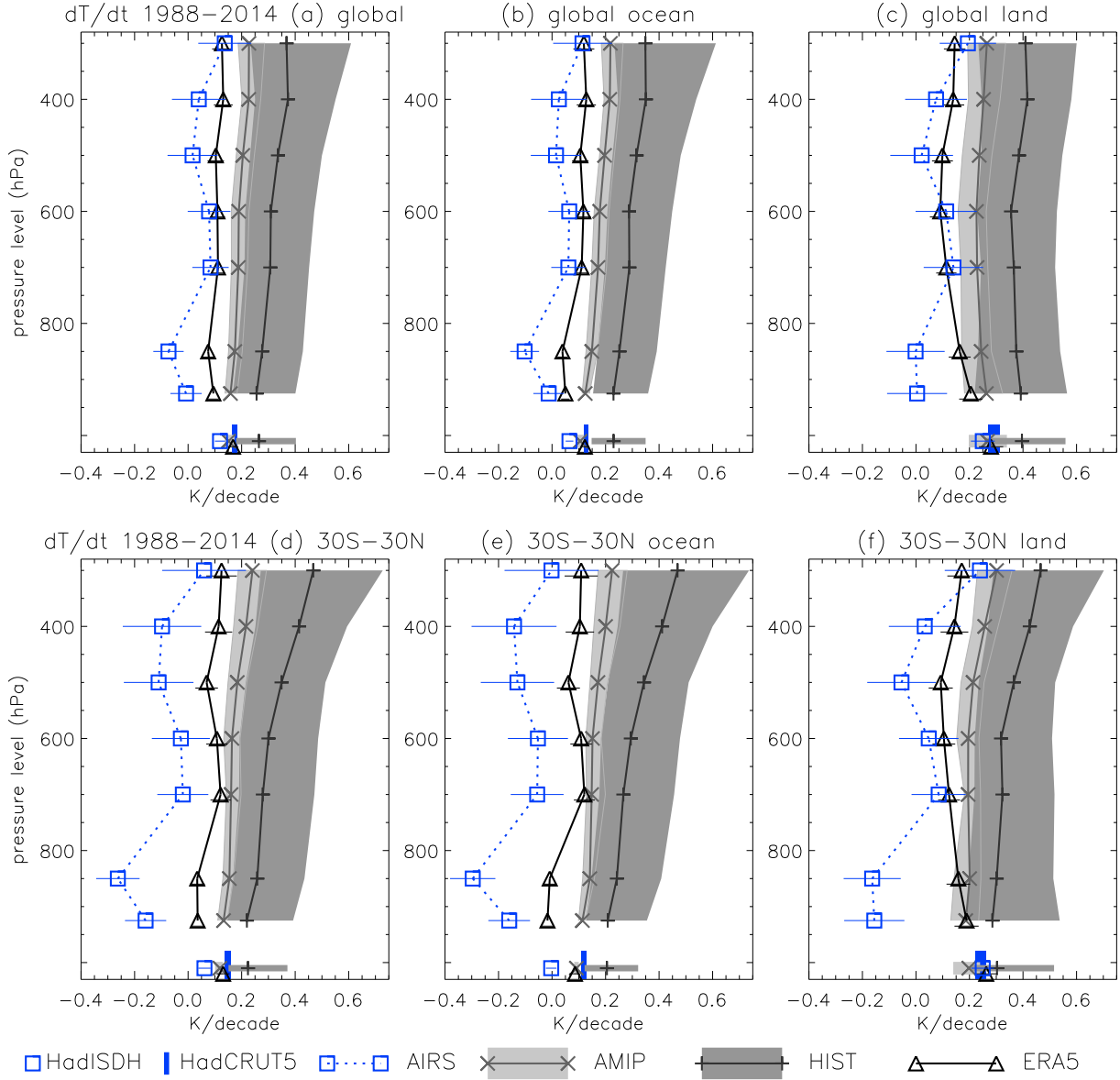
Figure S4. Trends in atmospheric and near surface temperature for the (a) global land and ocean, (b) global ocean, (c) global land, (d) tropical land and ocean, (e) tropical ocean and (f) tropical land over 1988-2014 for *amip* and *historical* model experiments (ensemble median±1 standard deviation), ERA5, AIRS satellite observations (2002-2014) and HadISDH 2 *m* observations

March 3, 2022, 3:50pm
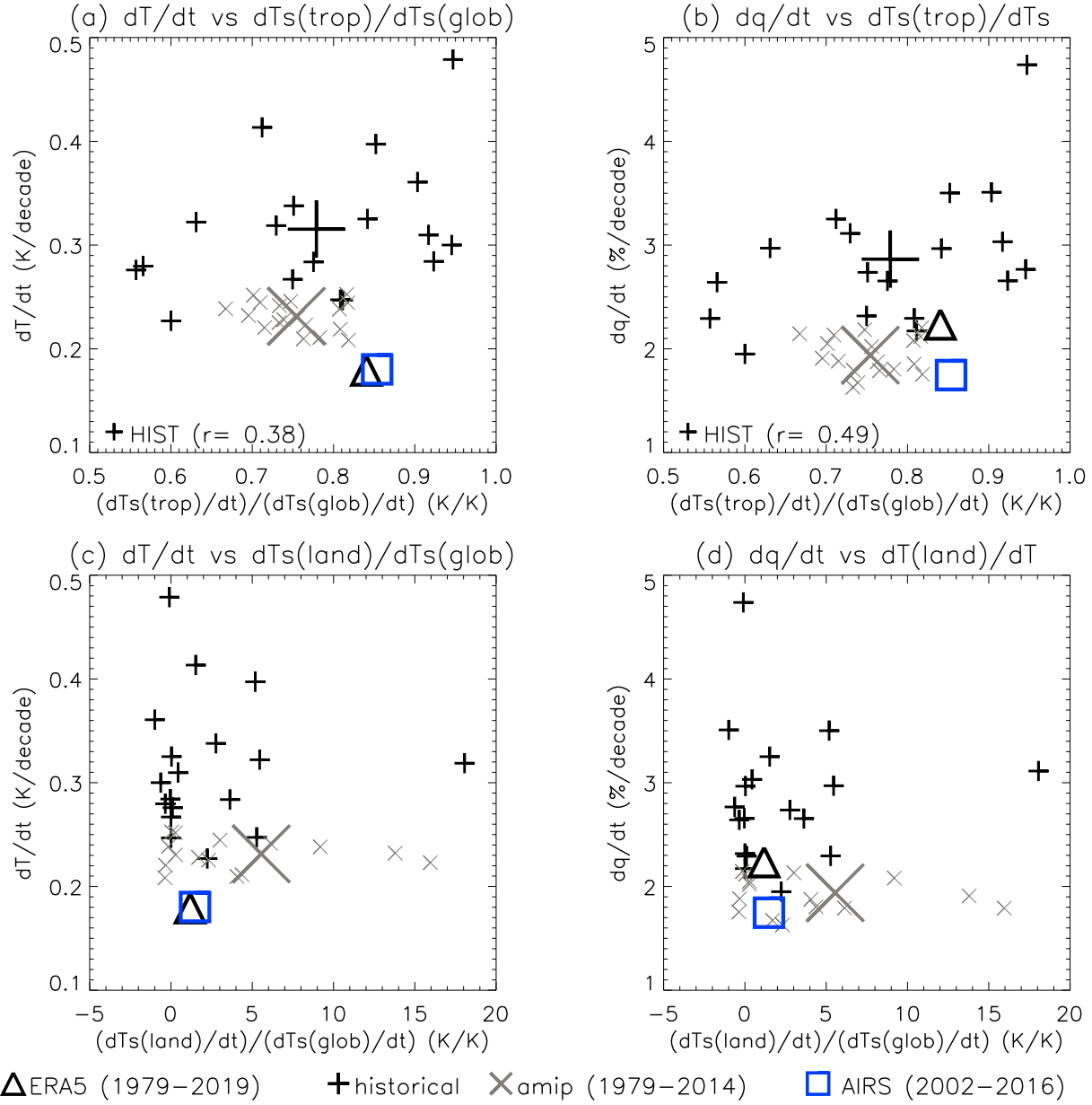
Figure S5. Relationships between trends in 400 hPa temperature (left column) or specific humidity (right column) and the ratio of trends in tropical to global surface temperature (a-b) or land to global temperature (c-d) for *amip* and *historical* model experiments (1979-2014; large symbols denote ensemble mean), ERA5 (1979-2019) and AIRS satellite observations combined with HadCRUT5 (2002-2016).

March 3, 2022, 3:50pm

Table S1. Global mean relative humidity (RH) and temperature (1995-2014) for model *amip* and *historical* experiments, ERA5 and observational-based estimates (HadISDH/ERA5 RH_{2m}; AIRS $RH_{700,400}$) and upper tropospheric humidity (UTH)* from HIRS and MW.

Model/*experiment*	RH_{2m} (%)		RH_{700} (%)		RH_{400} (%)		T_{700} (K)		T_{400} (K)	
	hist	*amip*	*hist*	*amip*	*hist*	*amip*	*hist*	*amip*	*hist*	*amip*
ACCESS-ESM1-5	77.5	77.8	45.9	46.7	42.1	42.4	275.3	274.5	248.7	248.0
BCC-CSM2-MR	—	—	51.6	52.0	48.0	48.35	274.2	273.8	247.4	246.8
BCC-ESM1	—	—	58.7	58.7	56.9	56.8	273.7	273.5	246.8	246.5
CanESM5	85.5	85.9	47.4	48.4	41.2	41.8	273.6	273.1	248.1	247.4
CESM2	77.6	78.1	52.3	53.8	48.4	49.2	274.1	273.2	247.7	246.7
CESM2-WACCM	77.7	78.2	52.5	54.0	48.7	49.4	274.0	273.2	247.7	246.7
CMCC-CM2-SR5	77.5	78.2	54.6	55.0	49.3	49.9	273.9	273.2	248.1	247.1
CNRM-CM6-1	75.8	75.8	55.6	55.3	54.1	54.2	271.6	272.3	243.8	244.7
CNRM-ESM2-1	75.6	75.5	55.6	55.4	54.0	54.2	272.2	272.3	244.4	244.7
GFDL-ESM4	—	—	—	—	—	—	273.4	273.6	246.5	246.8
GISS-E2-1-G	78.1	78.0	54.3	53.8	51.3	51.7	273.9	273.6	247.2	246.5
HadGEM3-GC31-MM	76.0	76.2	50.6	51.0	45.9	45.6	273.8	273.9	247.3	247.5
INM-CM5-0	76.0	75.9	51.1	51.5	50.1	49.3	273.2	274.2	246.1	247.6
IPSL-CM6A-LR	78.2	78.7	58.9	59.5	44.0	44.5	272.0	272.3	245.5	246.0
MIROC6	76.8	76.8	59.8	59.3	50.7	50.0	273.6	274.0	247.2	248.1
MRI-ESM2-0	79.4	79.7	52.0	52.7	51.2	51.4	273.5	273.7	246.9	247.2
NorESM2-LM	76.4	77.7	57.7	59.2	54.5	55.1	273.1	272.5	247.2	246.4
UKESM1-0-LL	76.0	76.0	51.4	51.7	47.5	47.3	273.4	273.7	246.9	247.2
Ensemble mean	77.6	77.9	53.5	54.0	49.3	49.5	273.6	273.4	246.9	246.8
Ensemble spread	±4.8	±5.0	±7.7	±7.3	±8.5	±8.3	±1.7	±1.3	±2.5	±1.8
ERA5	73.7		48.9		44.3		273.7		247.6	
HadISDH-ERA5, AIRS	74.5		47.3		41.0		274.1		247.6	
UTH (HIRS, MW)					25.5*, 33.3*					

Table S2. Global mean temperature trends (K/decade) (1988-2014) at 700 hPa and 400 hPa for model *amip* and *historical* experiments, ERA5 and observations-based estimates (AIRS 2002-2014) [*significant at 90% confidence level accounting for autocorrelation; ± 1 standard error in linear fit apart from model ensemble ± 1 standard deviation model spread.]

Model	T_{2m}		T_{700}		T_{400}	
Trend (K/decade)	*hist*	*amip*	*hist*	*amip*	*hist*	*amip*
ACCESS-ESM1-5	0.39±0.01*	0.14±0.01*	0.40±0.01*	0.18±0.01*	0.48±0.02*	0.21±0.02*
BCC-CSM2-MR	0.24±0.01*	0.14±0.01*	0.27±0.01*	0.18±0.01*	0.33±0.02*	0.22±0.02*
BCC-ESM1	0.25±0.01*	0.15±0.01*	0.27±0.01*	0.16±0.01*	0.31±0.02*	0.21±0.02*
CanESM5	0.37±0.01*	0.15±0.01*	0.45±0.01*	0.19±0.01*	0.55±0.02*	0.22±0.02*
CESM2	0.29±0.01*	0.15±0.01*	0.31±0.02*	0.20±0.01*	0.36±0.02*	0.26±0.02*
CESM2-WACCM	0.32±0.01*	0.16±0.01*	0.32±0.01*	0.19±0.01*	0.37±0.02*	0.24±0.02*
CMCC-CM2-SR5	0.36±0.02*	0.17±0.01*	0.38±0.02*	0.22±0.01*	0.44±0.02*	0.27±0.02*
CNRM-CM6-1	0.18±0.01*	0.16±0.01*	0.21±0.01*	0.17±0.01*	0.25±0.02*	0.22±0.02*
CNRM-ESM2-1	0.24±0.01*	0.14±0.01*	0.26±0.01*	0.16±0.01*	0.32±0.01*	0.20±0.02*
GFDL-ESM4	0.25±0.01*	0.14±0.01*	0.31±0.02*	0.19±0.01*	0.39±0.02*	0.25±0.02*
GISS-E2-1-G	0.22±0.01*	0.15±0.01*	0.26±0.02*	0.18±0.01*	0.35±0.03*	0.21±0.02*
HadGEM3-GC31-MM	0.38±0.01*	0.15±0.01*	0.39±0.01*	0.19±0.01*	0.46±0.02*	0.23±0.02*
INM-CM5-0	0.21±0.01*	0.16±0.01*	0.21±0.01*	0.19±0.01*	0.26±0.01*	0.23±0.02*
IPSL-CM6A-LR	0.22±0.02*	0.16±0.01*	0.25±0.02*	0.19±0.01*	0.33±0.02*	0.25±0.02*
MIROC6	0.25±0.01*	0.17±0.01*	0.31±0.02*	0.21±0.01*	0.39±0.03*	0.25±0.02*
MRI-ESM2-0	0.26±0.01*	0.15±0.01*	0.26±0.01*	0.19±0.01*	0.29±0.02*	0.22±0.02*
NorESM2-LM	0.30±0.01*	0.15±0.01*	0.35±0.02*	0.19±0.01*	0.43±0.02*	0.23±0.02*
UKESM1-0-LL	0.40±0.01*	0.15±0.01*	0.44±0.01*	0.19±0.01*	0.51±0.02*	0.22±0.02*
Ensemble median	0.26±0.07*	0.15±0.01*	0.31±0.07*	0.19±0.01*	0.37±0.09*	0.23±0.02*
ERA5	0.17*		0.11*		0.13*	
Observations	0.12*		0.08		0.04	

March 3, 2022, 3:50pm

Table S3.   Global mean atmospheric temperature sensitivity to surface temperature (K/K) (1988-2014) at 925 hPa, 700 hPa and 400 hPa for model *amip* and *historical* experiments, ERA5 and observations-based estimates (AIRS 2002-2014) [*significant at 90% confidence level accounting for autocorrelation; ±1 standard error in linear fit apart from model ensemble ±1 standard deviation model spread.]

Model	T_{925}		T_{700}		T_{400}	
dT/dTs (K/K)	*hist*	*amip*	*hist*	*amip*	*hist*	*amip*
ACCESS-ESM1-5	0.91±0.02*	0.88±0.02*	0.90±0.04*	0.98±0.05*	0.97±0.07*	1.12± 0.08*
BCC-CSM2-MR	0.98±0.02*	0.52±0.04*	0.94±0.04*	0.61±0.05*	1.03±0.07*	0.80±0.07*
BCC-ESM1	1.00±0.02*	0.91± .02*	1.03±0.05*	0.99±0.04*	1.15±0.07*	1.19±0.07*
CanESM5	0.98±0.02*	0.95±0.02*	0.95±0.04*	0.96±0.04*	1.04±0.06*	1.09±0.07*
CESM2	0.93± 0.02*	0.87±0.02*	1.03±0.05*	0.95±0.05*	1.28±0.07*	1.18±0.08*
CESM2-WACCM	0.89± 0.02*	0.88±0.02*	0.83±0.04*	0.89±0.05*	1.04±0.07*	1.04±0.07*
CMCC-CM2-SR5	0.98± 0.01*	1.02±0.02*	0.95±0.03*	0.95±0.04*	1.22±0.05*	1.06±0.07*
CNRM-CM6-1	0.91± 0.02*	0.87±0.02*	1.08±0.05*	0.96±0.04*	1.40±0.08*	1.17±0.06*
CNRM-ESM2-1	0.85±0.02*	0.85±0.02*	0.85±0.04*	0.97±0.04*	0.99±0.06*	1.20±0.07*
GFDL-ESM4	0.97±0.01*	0.88±0.02*	1.07±0.04*	0.96±0.05*	1.34±0.06*	1.10±0.08*
GISS-E2-1-G	0.92±0.02*	0.93±0.03*	1.09±0.04*	0.98±0.04*	1.68±0.07*	1.20±0.07*
HadGEM3-GC31-MM	0.87±0.02*	0.93±0.02*	0.95±0.04*	0.99±0.04*	1.14±0.06*	1.06±0.07*
INM-CM5-0	0.92±0.02*	1.01±0.02*	0.92±0.03*	0.91±0.04*	1.02±0.05*	1.02±0.06*
IPSL-CM6A-LR	0.89±0.01*	0.86±0.02*	0.94±0.03*	0.81±0.04*	1.18±0.05*	0.91±0.07*
MIROC6	0.95±0.02*	0.87±0.02*	1.52±0.04*	0.94±0.04*	2.00±0.07*	1.15±0.07*
MRI-ESM2-0	0.88±0.02*	0.87±0.02*	0.82±0.05*	0.78±0.04*	0.92±0.08*	0.85±0.06*
NorESM2-LM	1.00±0.02*	0.99±0.02*	1.00±0.04*	0.95±0.04*	1.22±0.06*	1.01±0.07*
UKESM1-0-LL	0.92±0.02*	0.91±0.02*	0.93±0.05*	0.97±0.05*	1.05±0.08*	1.10±0.08*
Ensemble median	0.92±0.05*	0.88±0.11*	0.95±0.15*	0.96±0.10*	1.15±0.27*	1.10±0.12*
ERA5	0.97*		1.00*		1.15*	
Observations	0.77*		0.96*		1.19*	

March 3, 2022, 3:50pm